Progress In Electromagnetics Research C, Vol. 61, 75–90, 2016

Flexible Antennas Based on Natural Rubber

Zaiki Awang[1, *], Nur A. M. Affendi[1, 2], Nur A. L. Alias[1], and Nur M. Razali[1]

Abstract—Flexible substrates have been increasingly studied in recent years. This paper proposes natural rubber as a new substrate material for flexible antennas. In our work, prototype antennas were built using rubber formulated with different filler contents. Carbon black was used as the filler where its amount was varied to yield different dielectric properties. Prototype inset-feed microstrip patch antennas with outer dimensions 7.52 mm × 10.607 mm × 1.7 mm and copper as its conducting material were fabricated to operate at 2.45 GHz. The prototypes were measured and their performance analyzed in terms of the effects of filler content on Q, return loss and bending effects on their gain and radiation characteristics. The return loss and gain were found to be comparable to those built on existing synthetic substrates, but these new antennas offer an added feature of frequency-tunability by varying the filler content. Under bending conditions, these new antennas were also found to perform better than existing designs, showing less changes in their gain, frequency shift and beamwidth, in addition to less impedance mismatch when bent.

1. INTRODUCTION

Although conformal antennas provide potential solution for many applications, compared to traditional rigid antennas, flexible antennas have some drawbacks whereby some of the characteristics change when the dielectric is stretched or compressed along their inner or outer surfaces. Bendable materials such as polydimethylsiloxane (PDMS), conductive fabrics, liquid metal alloys, polymers in paper [1–4] are widely used in current designs of flexible electronic devices. However, manufacturing complexities, high cost, poor electrical properties, and limited applicability for outdoor implementations are some of the complications which most existing flexible circuits face. Natural rubber, on the other hand, has a potential to be an alternative flexible material due to low production cost, ease of manufacturing, high elasticity and weather-proof, while offering stable electrical properties and quite importantly, being environmental-friendly.

The ease of varying the permittivity is also an added advantage for rubber. As reported by [5], the permittivity of PDMS can also be varied by inclusion of glass microsphere. However, the process is not straight-forward and difficult to control as possibility of broken glasses results in changes of the expected permittivity. In terms of high-volume manufacturing for rubber on the other hand, carbon black is more reliable filler than fragile glass microspheres.

Although rubber is a well-known material, their use in high frequency electronics has been limited, and to our knowledge, its implementation in microwave antennas has not been demonstrated thus far. There have been several reports on rubber previously but mostly have only focused on their dielectric [6–8] and thermo-mechanical [9] properties. There was an attempt to build antennas using EPDM rubber previously [10], but EPDM is synthetic rubber. To our knowledge, our work is the first attempt to demonstrate the use of natural rubber as a new material for flexible antennas. A first ever attempt of using natural rubber in flexible antenna design has been proposed by us previously in [11], in which

Received 25 September 2015, Accepted 16 December 2015, Scheduled 6 January 2016

* Corresponding author: Zaiki Awang (zaiki437@salam.uitm.edu.my).

[1] Microwave Technology Centre, Universiti Teknologi MARA, Shah Alam 40450, Malaysia. [2] School of Electrical System Engineering, Universiti Malaysia Perlis Kampus Pauh Putra, Perlis 02000, Malaysia.

computer simulations proved the viability of using this environmental-friendly natural material in flexible antenna design. Our study has shown in the paper that the antennas were able to operate almost as well as those using existing rigid and flexible substrates. In this paper, we conclude the study by reporting a full characterization of actual prototypes, including details of the fabrication processes involved, measurement of the dielectric properties of the substrates, and antenna characterization including the effects of filler content on antenna Q and the effects of bending on the return loss, radiation pattern, radiation efficiency and gain.

2. RUBBER FABRICATION

Compared to our previous paper [12], the rubber samples used in this latest work were prepared using a new improved filler formulation (CB N330) and with different filler contents varying from 0% to 60%. The rubber formulation was also new and included Standard Malaysian Rubber L (SMR L), zinc oxide, Antioxidant 2246 (2,2'-Methylenebis (4-methyl-6-tertbutylphenol)), sulphur and zinc diethyldithiocarbamane. The compounds were mixed using a two-roll mill. The process of cutting and folding the rubber composites helped in improving the dispersions of the compounds into the rubber matrix. Finally, 1.7 mm thick flat rubber sheets (shown in Figs. 1(a) and (b)) were produced after vulcanization in a compression mould. The samples were later subjected to microwave characterization to determine their dielectric properties.

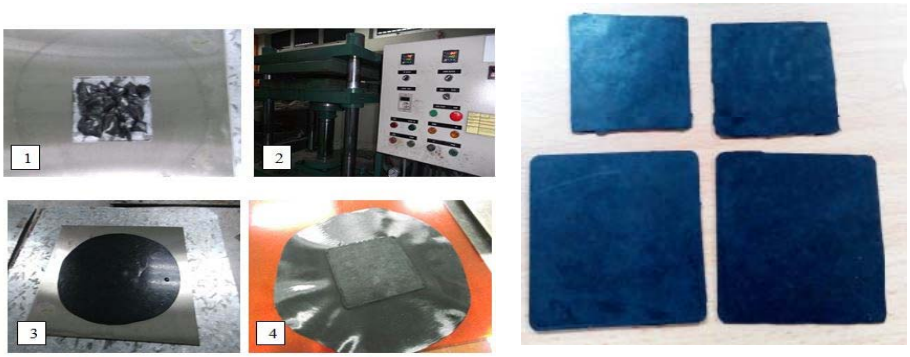

(a) (b)

Figure 1. (a) Rubber compound compressed at 140°C for 15 minutes using a customized moulding plate. (b) Rubber sheets produced after vulcanization.

3. MICROWAVE CHARACTERIZATION OF RUBBER

Designing rubber-based antennas require knowledge of the dielectric properties of the substrates at the intended frequency of use. There are several established techniques available to determine the dielectric properties of polymers, and several reports on the study of the dielectric properties of rubber appeared in the literature, conducted at various frequency ranges. Most involved the use of waveguide or probes [6, 7], including our work based on free-space non-destructive testing [12]. These are standard methods based on Von-Hippel. In this paper, the microwave properties of rubber were measured using the *Agilent 85070E* dielectric probe system, which employed a 3.5 mm-diameter coaxial probe. In selecting this type of probe we took precautions to ensure the sensing volume requirements were met so that the measurement errors were reduced. This condition requires that samples of certain thickness and size were used in the measurements [13]. In our case, all the rubber sheets were 1.7 mm thick (more than the minimum thickness required), and their sizes were large enough so that the probes were placed not less than 5 mm from the sample edges.

The ratio of the imaginary part to real part of the relative permittivity is called the loss tangent

$$\tan \partial = \frac{\varepsilon_r''}{\varepsilon_r'} \tag{1}$$

Figure 2 illustrates the variation of ε_r' with frequency for different filler contents measured in our work. From the observation, it can be seen that by increasing the filler from 0% to 60%, a significant change in ε_r' was obtained. The value increases with carbon content but decreases with frequency. The connectivity between filler particles and dipole interaction increased when the filler content increased, and this leads to the increase of relative permittivity of a material. The porosity of the natural rubber is higher than the carbon filled natural rubber because it is an amorphous material. Electromagnetic signals can move through the material easily, and less electric field energy can be stored in the material. Hence, this will lead to lower permittivity. The addition of carbon filler not only reinforces the composites, but also introduces electrical conductivity into rubber. This leads to an increase in the dielectric loss of the rubber since electrons easily shifted on the carbon black surface. This theory corresponds to the results that we have obtained in this work. As seen from the figure, the structure of the material becomes more compact and less porous as the amount of carbon black filler was increased.

Figure 3 plots the variation of ε_r'' against frequency. As seen from the figure, the increase in filler amount leads to a significant increase in $\tan\delta$. With higher filler contents, the effect becomes more noticeable. The fact that the addition of filler increases $\tan\delta$ implies that the material becomes more lossy thus leading to an increase in the electrical conductivity, in confirmation with [12]. Furthermore, the addition of carbon up to 20% weight can give a nine-order of magnitude increase in conductivity, ranging from 10^{-9} to 10 S/m [9]. Based on previous studies [8], a certain relaxation time is necessary since the polarization caused by the orientation of the dipoles cannot keep up with the fluctuating electrical strength. Therefore, since filler content influences the electrical conductivity and consequently

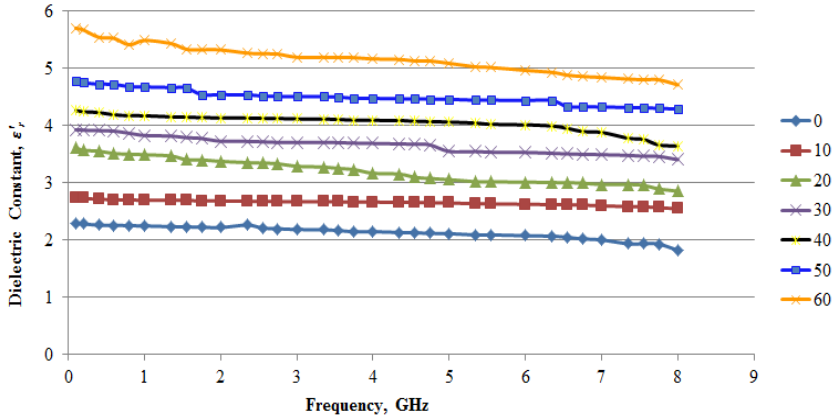

Figure 2. Frequency dependence of ε_r' with different filler content (%).

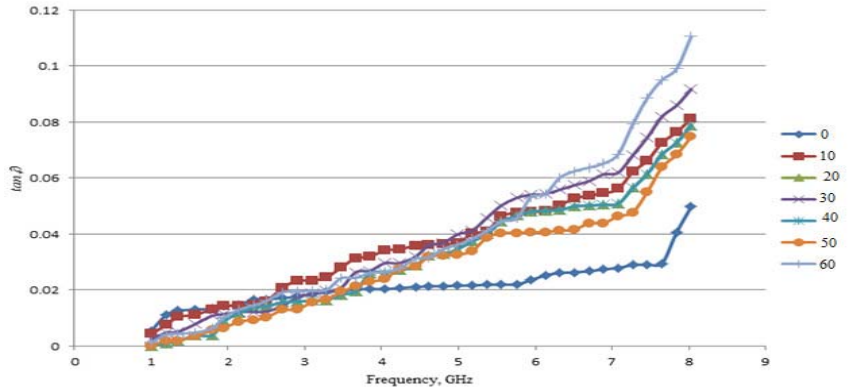

Figure 3. Frequency dependence of $\tan\partial$ with different filler contents (%).

the dielectric properties of the rubber, its subsequent effects on antenna quality factor Q, bandwidth and return loss are studied in this work.

4. ANTENNA DESIGN AND FABRICATION

4.1. Antenna Design

Several rectangular microstrip patch antennas were designed using natural rubber as the substrate using *CST Microwave Studio* software. This topology was chosen due to its simplicity to prove that rubber can be used as a substrate for the flexible antenna. Each antenna had the same patch dimensions, but used substrates of different filler contents (corresponding to different permittivity). The idea was to fix the patch dimensions while varying the filler loadings, so that the effect of filler content on the resonance frequency can be studied. Table 1 lists the antenna dimensions, calculated using the transmission line model, and based on substrate permittivity and loss tangent of 3.1 and 0.02 (corresponding to 10% filler content) respectively. The antenna geometry is shown in Fig. 4. In order to match the radiating patch to the line, the patch was fed from the edge using an inset microstrip line. This feeding method sets the line impedance at 50 Ω by cutting a narrow notch out of the radiating edge far enough into the patch to give the required driving point impedance.

Table 1. Dimensions of the rectangular microstrip patch antenna (all dimensions are in mm).

Patch length L_p	7.52
Patch width W_p	10.607
Ground length L_g	50
Ground width W_g	50
Inset feed length L_{fi}	7.5
Inset feed width W_{fi}	1.5
Feed length L_f	32
Feed width W_f	3.8
Substrate thickness h	1.7

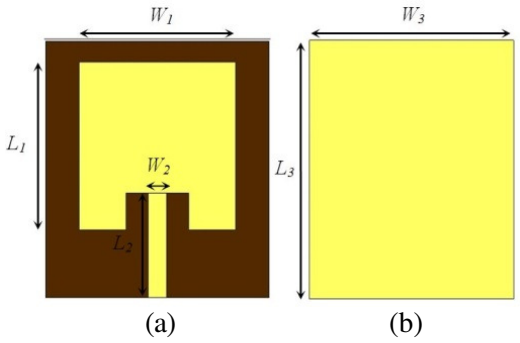

Figure 4. (a) Front and (b) back views of the antenna.

4.2. Prototype Fabrication

Copper sheets were used as the conducting material of the antennas; the sheets were cut using an industrial cutter to give the patch shape. The copper was 0.15 mm thick as available in the market. Two types of industrial adhesives (*CHEMLOK 205* and *220*) were applied on one side of the copper in order to create good adhesion between the copper and rubber surfaces. Rubber sheets were prepared

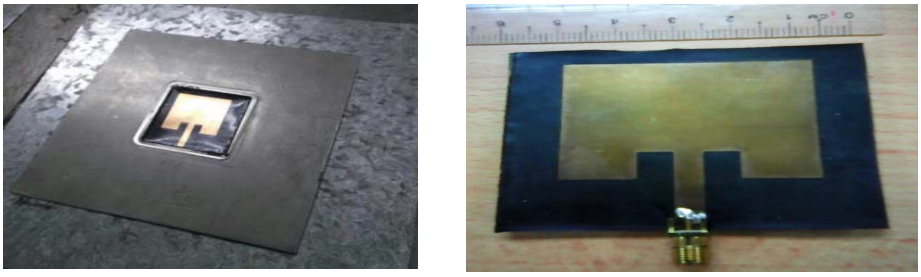

(a) (b)

Figure 5. (a) A custom-made plate for the hot press process and (b) prototype antenna.

by fitting rubber compounds in a moulding plate with thickness of 1.7 mm before undergoing hot compression at 140°C for 10 minutes. Excess rubber was removed off the edges before the copper sheets were secured onto the rubber surfaces, and this then underwent hot compression for another 5 minutes (Fig. 5(a)). A 50 Ω SMA connector was then soldered to the antenna after it was let to cool to room temperature (Fig. 5(b)).

5. RESULTS AND DISCUSSIONS

5.1. Effects of Filler Content on Antenna Quality Factor

To study the effects of filler content on antenna performance, each antenna was simulated using different filler loadings but with fixed antenna dimensions. Four equal-sized antenna prototypes designed in the previous section were simulated using *CST Microwave Studio* to predict and analyze the filler effects on the antenna performance. Figs. 6 and 7 show the simulated and measured responses of the antennas respectively. The measured responses were obtained from antennas located in free space connected to a vector network analyzer and calibrated using Short-Open-Load-Through (SOLT) calibration. The following deductions can be made:

i. The bandwidth increases with filler content. There is a gradual widening of the return loss traces at resonance as the filler was increased from 10 to 40%. As the filler content increases, $\tan\delta$ increases — the substrate thus becomes more lossy, and Q decreases. This leads to a widening of the return loss trace on the graph.

ii. The return loss (and thus antenna matching) are highly influenced by filler content. This is due to the fact that the filler amount would affect the substrate permittivity, and thus the characteristic impedance of the lines change, leading to a change in the impedance match in the process.

iii. The resonant frequency is also affected by filler content. This shift in frequency is explained by the fact that as the permittivity changes, the signal wavelength changes too, giving rise to a shift in the frequency as shown. It is thus possible to tune the operating frequency without changing the antenna dimensions — this an advantage for applications in which size adjustment of antenna is a constraint.

The antennas are analyzed based on the return loss and bandwidth. A good agreement of the bandwidth is achieved between simulation and measurement — the bandwidths increased as $\tan\delta$ increased. This behavior can be explained by the following theoretical analysis. The total Q of an antenna is given by (2);

$$\frac{1}{Q} = \frac{1}{Q_{rad}} + \frac{1}{Q_c} + \frac{1}{Q_d} + \frac{1}{Q_{sw}} \tag{2}$$

where Q_{rad}, Q_c, Q_d and Q_{sw} are the quality factors for radiation or space wave, conductor, dielectric and surface wave, respectively. The dielectric quality factor Q_d is inversely proportional to $\tan\delta$ through Eq. (3) [14, 15];

$$Q_d = \frac{1}{\tan\delta} \tag{3}$$

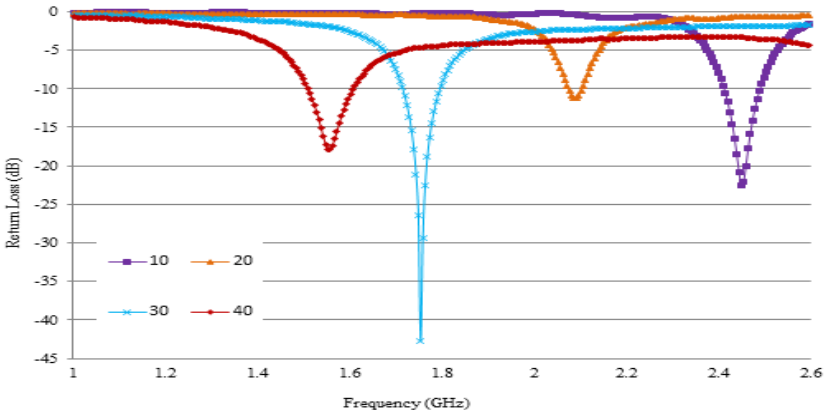

Figure 6. Simulated return loss of equal-size antennas with different filler content. As the filler loading (%) increases, the resonance frequency decreases.

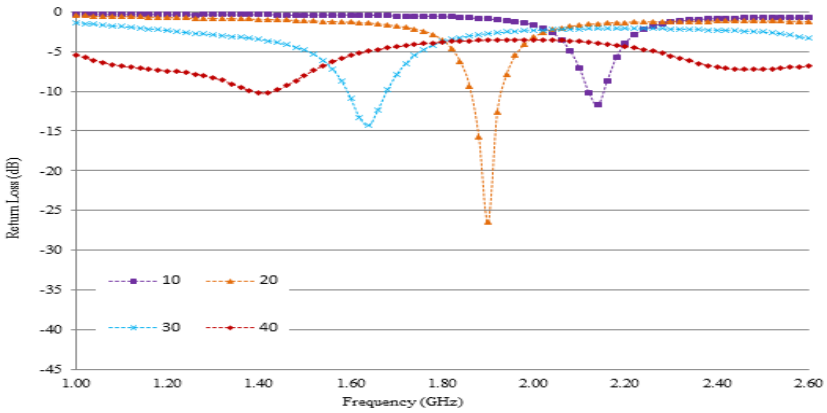

Figure 7. Measured return loss of the equal-size antennas with different filler loadings (%) showing the same inverse dependency of the resonance frequency f_r with filler content.

The increases of filler content cause the electrical conductivity and consequently $\tan\delta$ to increase. From Eq. (3), this leads to a decrease in Q. Since the bandwidth is inversely proportional to Q as seen in Eq. (4) below [16, 17];

$$BW = \frac{VSWR - 1}{Q\sqrt{VSWR}} \tag{4}$$

it follows that the antenna bandwidth is enhanced with the filler content, as observed from the prototypes. In Eq. (4), BW is the antenna bandwidth, while VSWR is the voltage standing wave ratio. Thus it can be concluded that as filler increased, the bandwidth increases too since the substrate becomes more lossy.

Figure 8 shows comparison between simulated and measured return losses. There are some frequency shifts seen between the two sets of data — the shift could have been due to the following possibilities:

i. The substrate permittivity could have changed resulting from hot compression where a temperature of 140°C was applied to aid adhesion of Cu to the rubber surface, while also vulcanizing the rubber. This is because the electrical properties of dielectrics are generally dependent on frequency, temperature, and surface roughness [18]. In fact, in the course of our work, we did measure the effects of heat on permittivity and this was confirmed. Therefore, the effects of temperature during vulcanization of rubber should be considered before characterizing its dielectric properties.

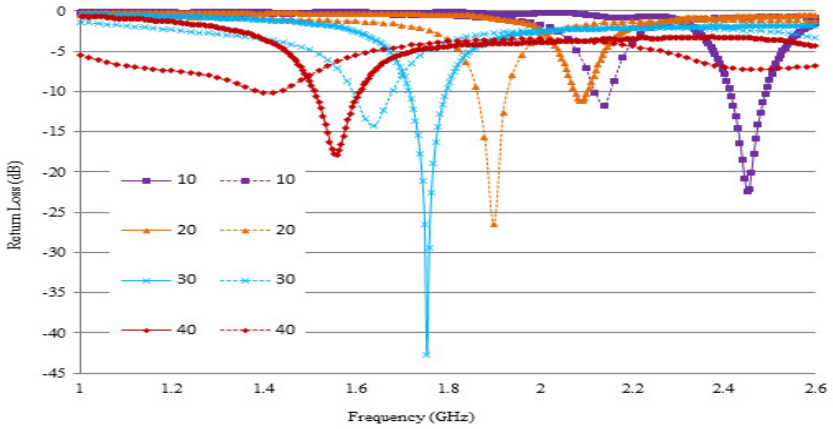

Figure 8. Comparison between the simulated (solid lines) and measured (dashed lines) return loss of prototype antennas of different filler content (%).

ii. The shift may also be attributed to the difference in the patch length since the operating frequency f_r of the antenna is a function of its length, L_p [19] as related by (5):

$$f_r = \frac{c}{2L_p\sqrt{\varepsilon_{eff}}} \tag{5}$$

where c is the speed of light in free space and ε_{eff} the effective permittivity. Measurements using a precision travelling microscope on our samples revealed the antenna patch increased by about 0.5 mm. This could have lowered f_r by about 11%. We believe that the slight change in the patch dimension was due to mechanical imprecision of the cutter used and that the change did not occur during the processes followed. In practice, precision metal cutters should be utilized to reduce this discrepancy. It can be seen, however, that the general trend of the frequency response and bandwidth are in good agreement with simulation.

Table 2 shows the bandwidth, return loss and Q obtained from the simulation and measurement. From the tabulated data, the bandwidth of the antennas improved as Q is decreased. This is due to increase of $\tan\delta$ as supported by our studies previously. The bandwidths of our prototypes compare favourably with the designs of other workers using synthetic materials such as paper, polymers and textile-based wearable designs [2, 20, 21]. However, the measured return loss was degraded except for antennas with 20% filler. Measurements of the patch dimensions using a microscope revealed slight reductions of the feedline width and length (up to 0.1 and 0.8 mm respectively) of the prototypes, thus affecting the impedance matching and therefore increasing the return loss. Also, oxidation and imperfections of the Cu sheet could also affect the radiating efficiency of the antenna. These sample defects could have been brought about by the thermal compression. Additional losses could result from this thermal process too, since the conductivity of the material is reduced, and therefore lowering the efficiency of the antennas. It should be pointed out that the heating was applied when the copper sheets were pressed to the rubber sheets to ensure the patch is secured properly. The heating was only applied at this stage and not at other stages, to ensure the effect of heat on the dielectric properties of the rubber substrates was minimized.

The return loss of antenna with 20% filler improved however. The measured feedline width and length were 4.823 and 24.17 mm, respectively. The improvement of the return loss suggests that the impedance matching of the antenna was good for the stated dimensions. Therefore, it is crucial that precise dimension of the antenna is maintained, in addition to the metallization quality, as they can affect the antenna performance. Since this is our first attempt in constructing flexible antennas using natural rubber, other alternatives will be investigated to improve the patch and ground metallization in future works.

Table 2. Comparison between simulated and measured bandwidth, return loss and Q of the prototype antennas.

Filler Content (%)	Simulate			Measured		
	BW (%)	RL (dB)	Q	BW (%)	RL (dB)	Q
10	5	−22.49	20	2.82	−11.72	35.46
20	3.75	−11.16	26.67	5.29	−26.50	18.9
30	7.8	−42.75	12.82	11.04	−14.30	9.06
40	12.8	−17.89	7.81	40	−10.21	2.5

5.2. Bending Formulation of the Designed Antenna

To study the effects of bending, now the resonance frequency was fixed. A prototype that operated at 2.4 GHz was chosen for this purpose. The effect of bending on the proposed antenna is studied at two different bending directions — E- and H-planes shown in Figs. 9(a) and (b) respectively. The simulation model of the bendable antenna is designed using the afore-mentioned software. This model permits prediction of the antenna performance when it is subjected to bending. To quantify the bending, a bending angle θ is defined in Fig. 9. By this definition, a flat antenna implies θ is 180°, and that smaller bending angles imply higher amount of bending.

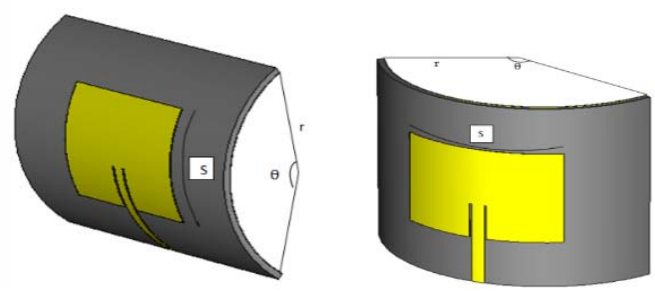

(a) (b)

Figure 9. Definition of the bending angle θ.

For both bending planes, the antenna was subjected to bending at two different bending angles θ namely 60° and 160°. By changing the bending angle, the cylinder radius changes too. The formula used to find out the radius of the cylinder that corresponds to the bending angle is shown below [22]:

$$S = r\theta \tag{6}$$

where S is the arc length, r is the radius of the cylinder and θ the bending angle in radians.

For the antenna bent around the H-plane, the antenna width was used as the arc length while for the antenna bent around the E-plane, the antenna length was used.

5.2.1. Flat Conditions

The S-parameters were measured using a *Rohde & Schwarz* vector network analyzer over the frequency range of 1 to 3 GHz at 500 MHz intervals. As can be seen in Fig. 10, the simulated response shows close agreement with the measurement, with similar behavior right across the measurement range. The resonance frequency deviated slightly to 2.39 GHz from the predicted 2.45 GHz, a shift of 2.4%. The measured return loss increased by 2 dB to −22 dB. One possible reason for this discrepancy could be due to tolerances of the fabrication process. During the fabrication, bonding agents are used to bond the copper sheets to rubber. The presence of the bonding agents causes an additional increase in the

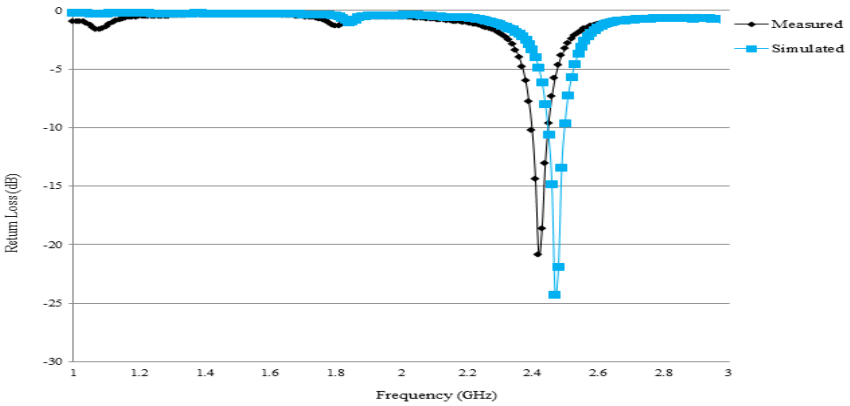

Figure 10. Measured and simulated return loss of the antenna under flat conditions.

overall thickness of the antenna. According to [11, 23], the fringing effect will be increased with the substrate thickness which causes the resonance frequency to decrease. Moreover, during the bonding process, slight misalignment could have occurred between the bonding layers. This could lead to some inaccuracies in terms of the antenna dimensions. The addition of bonding agents would also have altered the permittivity of the substrate structure, thus affecting the antenna response in turn. During the simulation these factors were not considered, and hence could have given rise to some discrepancies between the two sets of data. Despite that, the antenna still exhibited reasonable return loss at the intended frequency, fulfilling the requirements for good antenna operation. The frequency shift is quite small however, and in actual use could be easily tuned out to offset the shift.

5.2.2. Bent Conditions

One of the unique features of a flexible antenna is its bendability. A good flexible antenna should be able to offer acceptable performance even when it is bent. For this, the effect of bending on these new rubber-based antennas need to be investigated. The resonant frequency and return loss must be evaluated under several bending conditions since these properties are affected by geometrical changes of the circuit which may occur during bending. This is due to the impedance mismatch and change in the effective electrical length of the radiating elements.

The measurement set-up to measure the effect of bending on return loss is shown in Fig. 11. The antennas were mounted on cylindrical PVC pipes of different radii to imitate different bending angles. The PVC pipes allow the antennas to be bent in E- and H-planes as required. The same set-up was used for radiation pattern measurements.

Figure 12 is a plot of the measured return losses under H-plane bending. As expected the resonance frequency shifted slightly to a higher value as the antenna is bent along this plane. The effect of bending on the resonance frequency is predicted by the equation below [24]:

$$f = \frac{1}{2\sqrt{\mu\varepsilon}}\sqrt{\left(\frac{m}{2\theta a}\right)^2 + \left(\frac{n}{2b}\right)^2} \tag{7}$$

where f is the resonant frequency, b is the patch length, a the cylinder radius, and θ the bending angle in radians. m and n are the propagating modes, and ε and μ are the substrate permittivity and permeability, respectively.

This equation indicates that for an antenna of given ε and μ radiating at mode m and n, changes in the resonance frequency are mainly attributed to the patch length, which is a direct result of the bending. From Fig. 12 we see that the resonance indeed shifted higher as the bending angle decreased. Our work concurs with that reported by Bai and Langley [25] which observed a similar increase in the resonance frequency as the antenna was increasingly bent along the H-plane — this was explained by the fact that with increased bending, the resonant length is reduced further, hence increasing the resonance frequency.

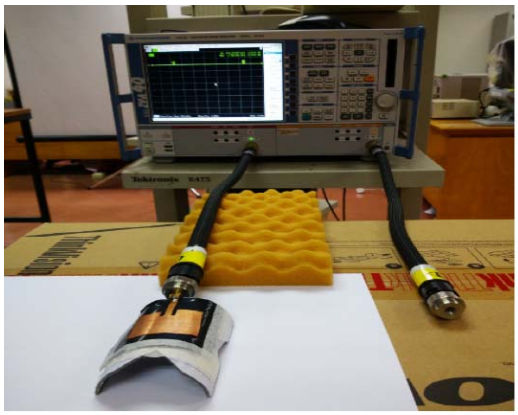

Figure 11. Bending test set-up.

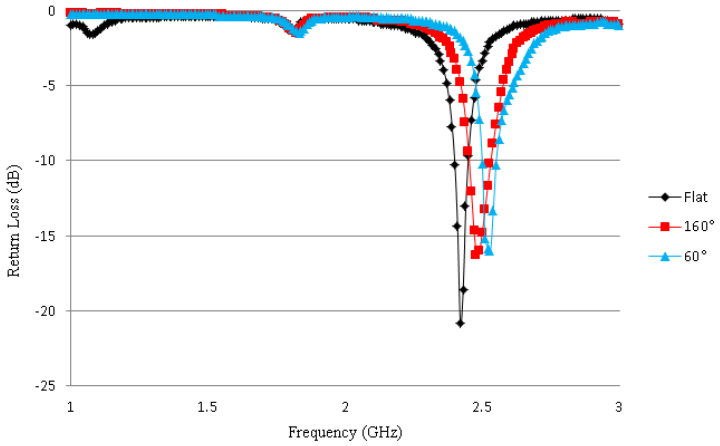

Figure 12. Measured return losses of the antenna at different H-plane bending angles.

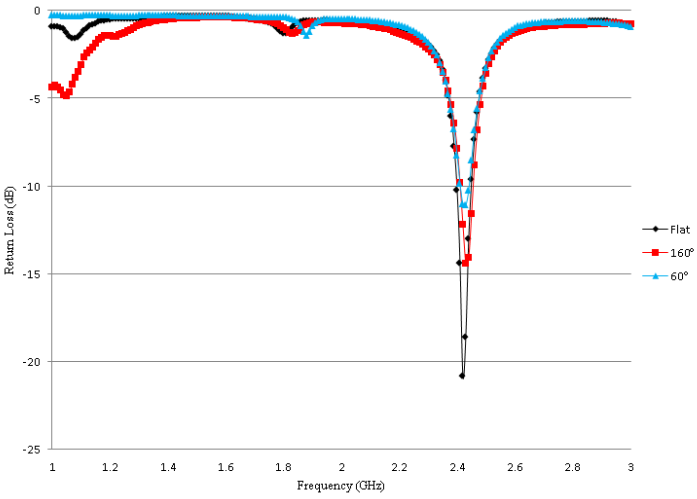

Figure 13. Measured return losses of the antenna at different E-plane bending angles.

Figure 14. Radiation pattern measurement set-up inside the anechoic chamber.

Figure 13 shows the return loss curves for E-plane bending. As indicated by the results, the resonance frequency is nearly unchanged as the antenna is bent along this plane. They remain very close to 2.45 GHz for both bending angles (60° and 160°). However, the return loss increased as the bending angles decreased. At 160°, the return loss at resonance was −14.3 dB, but this increased to −12 dB at 60°. This implies the match degraded with bending. As we bent the antenna along the E-plane, the patch width tends to elongate more than when it is flat. Since the impedance is affected by the patch width, increasing its dimension will result in a change in the impedance. As a result, mismatch occurs resulting in the increase of return loss.

Table 3 summarizes the results of Figs. 12 and 13 in terms of the resonance frequency, return loss and bandwidth. It can be observed that E-plane bending has minor effects on the antenna resonance frequency compared to H-plane bending. This is due to the fact that H-plane bending affects the antenna resonance length. The more the antenna is bent, the more resonance length is reduced, and thus the frequency increases. Bending in the E-plane on the other hand, seemed to affect the return loss and bandwidth of the antenna more. For both E-plane bending angles, the return loss increased between 7 to 10 dB. As stated previously, when the antenna was bent, the mismatch increased.

Table 3. Summary of the measured antenna response affected by bending.

Bending condition		Resonance frequency (GHz)	Return loss (dB)	Bandwidth (MHz)
Flat		2.45	−22	128
H-plane bending	$\theta = 160°$	2.485	−17	152
	$\theta = 60°$	2.52	−16	155
E-plane bending	$\theta = 160°$	2.46	−14.3	131
	$\theta = 60°$	2.46	−12	148

5.3. Radiation Pattern Measurement

The far-field radiation patterns of the antenna were measured in a fully equipped anechoic chamber. The AUT was placed on a positioner and aligned to a horn antenna having a standard gain. The measurement set-up is shown in Fig. 14.

5.3.1. Flat Conditions

The simulated and measured radiation patterns of the antenna at the resonance frequency under flat condition are shown in Fig. 15. It can be seen that the antenna radiates power equally in the front direction; there are no side lobes observed. Two back lobes began to appear pointing in the same direction as predicted from the simulation. The measured back lobe power levels are higher than simulation — this is quite common for non-coaxial fed antennas where isolation from the back side is quite poor. The antenna achieved a measured gain of 2.3 dB which fairly agrees with the simulated value of 2.49 dB. The response is what one could generally expect from the usual microstrip patch antenna built on rigid substrates. This again proves that natural rubber can be used as an alternative substrate.

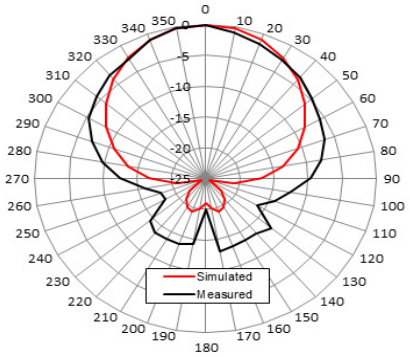

Figure 15. Measured and simulated radiation patterns of the antenna for flat condition.

5.3.2. Bent Conditions

The radiation patterns measured at resonance for two different bending planes are plotted in Figs. 16 and 17, respectively. They are both compared with simulation as shown. It was observed that the predicted and measured curves agree well-there is no distinct difference between the shapes of the patterns and their main and back lobes are pointing in the same direction. Good agreements between them prove the validity of simulations over the whole band. As seen from the measurement, back lobes existed as predicted from the simulation shown. The measured patterns are wider than simulation — this could have been due to errors in modeling the antenna in the simulation. Inaccuracies in the material properties of the antenna parameters used could have led to the slight widening of the measured radiation pattern.

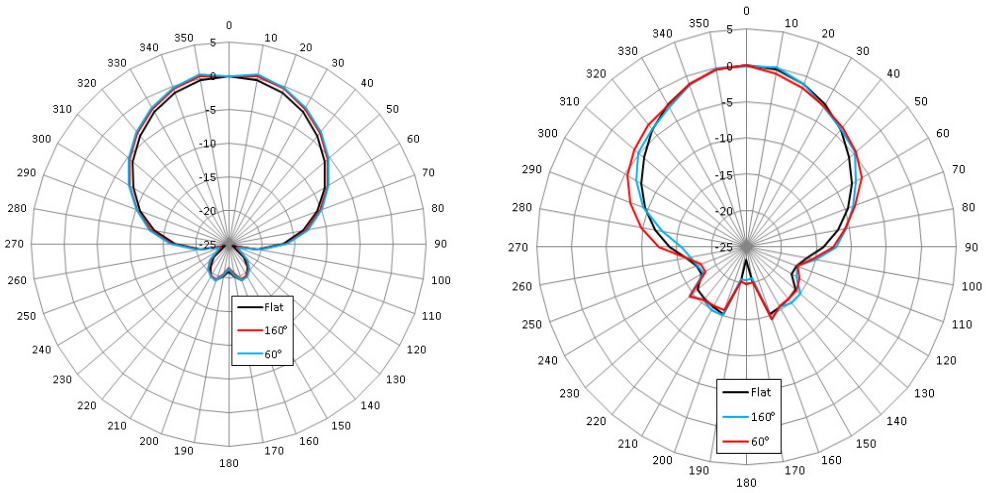

(a) (b)

Figure 16. (a) Simulated and (b) measured radiation patterns of the antenna bent along the E-plane.

Figure 16 shows bending in the E-plane. As mentioned before, as we bend the antenna along this plane, the patch width changes. Since the patch width has a minor effect on the radiation pattern [26], bending along this plane therefore has almost no influence on the patterns. The data in Table 4 proves these observations since there are no severe variations in the 3 dB beamwidth as the antenna was bent further. Considering the gain of the antenna as tabulated in Table 6, it is encouraging to note the antenna still showed acceptable gain even when bent down to 60°. Hence, it can be concluded that the antennas performed reasonably well when they are subjected to bending along the E-plane.

Table 4. Main lobe 3 dB beamwidth measured for flat and different angles of E-plane bending.

Bending angles θ (°)	**3 dB Beamwidth (°)**	
	Measured	**Simulated**
Flat	63	60.2
160	63.2	61
60	64	63

Figures 17(a) and (b) show the simulated and measured radiation patterns of the antenna under H-plane bending. For both cases of H-plane bending, the patterns widened with bending. The data in Table 5 prove these observations since the 3 dB beamwidth increased with bending. This effect is rather expected because the antenna has to adapt to the bending by altering the patch shape when stretched. The elongated shape may result in the face of the patch pointing in slightly broader directions, allowing for wider pattern as bending increased.

Besides that, as an antenna is bent, the effective dielectric constant ε_{reff} has been found to increase [22]. This behaviour is described by the following equation.

$$\varepsilon_{rcomp} = \varepsilon_r \left(1 + \eta \frac{h(d-0.5)}{a}\right) \tag{8}$$

where η is the proportionality factor, h the substrate height, d the diameter of the cylinder, a the cylinder radius, ε_r the permittivity of the substrate under flat condition, and $\varepsilon_{r,comp}$ the permittivity of the substrate when it is bent. With increasing ε_{reff}, more energy is radiated in the broadside direction as the number of modes guided in the substrate increases [27]. Hence, wider patterns are observed.

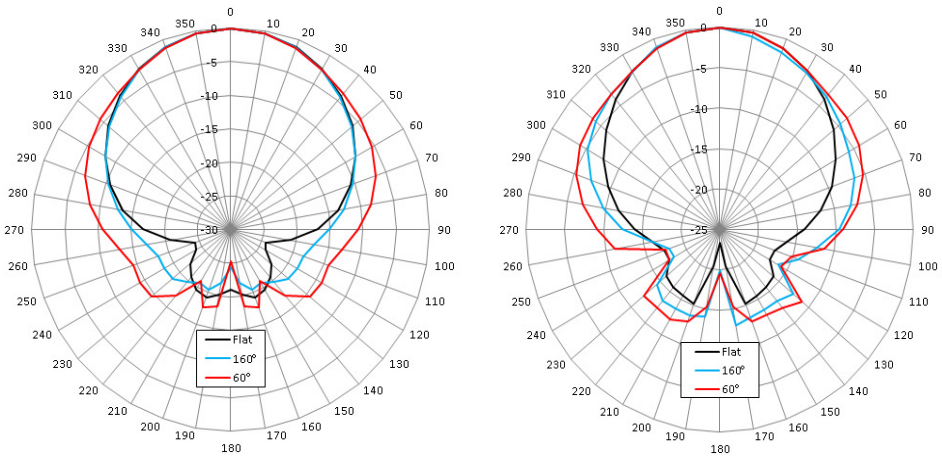

(a) (b)

Figure 17. (a) Simulated and (b) measured radiation patterns of the antenna bent along the H-plane.

Table 5. Main lobe 3 dB beamwidth measured for flat and different angles of H-plane bending.

Bending angles θ (°)	**3 dB Beamwidth (°)**	
	Measured	**Simulated**
Flat	63	60.2
160	75	69
60	80	74

Table 6 tabulates the directivity, gain and radiation efficiency of the antenna bent along both planes. It can be observed that the results for E-plane bending follow a slightly different trend then for H-plane. There are no severe variations in the gain, directivity and radiation efficiency as the antenna is more bent in E-plane. This is due to the fact that E-plane bending only affected the patch width which has a minor effect on the radiation pattern. However, as the antenna is bent along the H-plane, the main lobe broadens, and this translates to a drop in gain and directivity. The broadening of the patterns is thought to be due to increasing ε_{reff} when bent.

Table 6. Comparison between antenna radiation characteristics measured for flat and different bending conditions.

Bending condition		**Gain (dB)**	**Directivity (dBi)**	**Radiation efficiency (%)**
Flat		2.3	6.51	30.5
H-plane bending	$\theta = 160°$	1.7	6.3	27.2
	$\theta = 60°$	1.6	5.9	26.3
E-plane bending	$\theta = 160°$	2.1	6.48	28.8
	$\theta = 60°$	1.9	6.35	27.9

5.4. Comparative Study

The performances of our antenna prototypes were compared to other flexible antennas reported in the literature [21, 28–30], their principal features are tabulated in Table 7. The chosen antennas all had the same topology, and operated at 2.45 GHz. The key parameters chosen for comparison were compactness (i.e., size and thickness), the dielectric properties and their performances under bending.

Table 7. Comparative study of different types of flexible antennas.

Characteristics		Proposed antenna			Textile antenna [21]				PTFE [28]			PDMS [29]		Polyacrylate [30]		
Dielectric properties		$\varepsilon_r = 3.1$; $\tan\delta = 0.02$			$\varepsilon_r = 1.44$; $\tan\delta = 0.01$				$\varepsilon_r = 1.96$			$\varepsilon_r = 2.65$; $\tan\delta = 0.02$		$\varepsilon_r = 1.38$; $\tan\delta = 0.02$		
Substrate height h (mm)		1.0			2.85				1.27			2		1.36		
Metal thickness t (mm)		0.15			0.5				Not specified			0.025		Not specified		
Size $L \times W$ (mm)		32×40			47.9×55.43				42×43			45×35.5		50×60		
Radiating element material		Copper sheet			Copper sheet				Copper sheet			Graphene sheet		Copper foil tape		
Substrate		Natural rubber			Polyester and cotton				PTFE			PDMS *Sylgard* 184		Polyacrylate		
Antenna performance	Bending angles θ (°)	180	160	60	180	63	50	36	180	150	60	180	75	180	73	51
	Resonance frequency f_r (GHz)	2.45	2.46	2.46	2.43	2.5	2.5	2.6	2.45	2.46	2.47	2.45	2.46	2.44	2.49	2.51
	Return Loss (dB)	−22	−14	−12	−18	−16	−14	−12	−30	−14	−8	−55	−22	−17	-	-
	Gain (dB)	2.3	2.1	1.9	9.62	-	-	-	-	-	-	4.88	4.73	7	6	5
	3 dB beamwidth (°)	63	63.2	64	62	61	65	67	70	90	96	-	-	-	-	-

Note that textile-based antennas [21] showed the highest gain during flat condition — this was expected since textiles have lower permittivities thus giving higher gains since the gain of microstrip antennas varies inversely with ε_r. Our antennas exhibited the highest ε_r among those compared, and thus lower gain was obtained. Being less compact, textile materials contain more air space which lower the permittivity. Textiles also exhibit lower loss tangent values than rubber-based antennas, and are thus less lossy. Rubber antennas on the other hand are more lossy (due partly to the way they are prepared) and this led to more dissipation of the electromagnetic energy in the material, thus lowering the gain. With improved preparation techniques, rubber substrates having lower ε_r and loss tan should be possible, and antennas with improved all-round performance are a possibility.

Under different bending conditions, all antennas showed a drop in their gains, while the return loss degraded. Their 3 dB-beamwidths increased with bending, as it should. The effects of bending on the resonance frequency and return loss of the antennas have also been compared. The trends of our results correlated with others — as the antennas were bent, the resonance frequency shifted up and the return loss degraded. As we can see, the largest frequency shift (about 170 MHz) was observed with textile-based antennas, while those built from PTFE, PDMS and rubber showed the least frequency shift of only about 10 MHz. On the other hand, PDMS-based antennas exhibited the worst degradation in the return loss (about 33 dB), while that of our antenna only worsened by about 10 dB. Our antennas were subjected to more acute bending however, and yet only suffered minimal reduction in gain and demonstrated lower increase in the beamwidth. These features make rubber antennas more attractive since their performance is less affected by the conditions where they are installed in practice.

In summary, our antennas showed acceptable performance, by exhibiting characteristics comparable with, if not better than, those built on rigid substrates when flat. Our antennas also demonstrated good behavior under bent conditions — rubber being naturally flexible, our antennas were the least affected by bending. Due to the higher ε_r, our antennas were more compact and thinner than others. Also, the dielectric properties of rubber are easily controlled, and this is a definite advantage over other substrates. Thus, with more elaborate antenna designs and improved processing conditions, rubber-based antennas with better gain is possible.

6. CONCLUSIONS

This paper has presented a detailed study on flexible antennas built from a new substrate. Several prototypes were successfully built and their performance investigated. Their full results are reported here for the first time. The effects of filler loading on the antenna quality factor and bandwidth were observed. The filler amount affected the performance as expected, and some frequency tuning was possible with filler loading. With improved processing techniques, it should be possible, in theory, to produce rubbers with better dielectric properties, and consequently antennas with better performance should be realizable.

The antennas were also studied at two different bending directions — E- and H-planes. Based on the observations, we found that H-plane bending appeared to have more effect on the antenna performance than E-plane one. However, it is worth to mention that the antennas performed better when they were subjected to bending than antennas with other substrates. Therefore, we have proved the feasibility of using a new natural material in designing bendable antennas.

ACKNOWLEDGMENT

The project was supported by the Ministry of Science, Technology and Innovation, Malaysia under the Science Fund research grant scheme.

REFERENCES

1. Liyakath, R. A., A. Takshi, and G. Mumcu, "Multilayer stretchable conductors on polymer substrates for conformal and reconfigurable antennas," *IEEE Antennas and Wireless Propag. Lett.*, Vol. 12, 603–606, 2013.
2. Hayes, G. J., A. Qusba, M. D. Dickey, and G. Lazzi, "Flexible liquid metal alloy (EGaIn) microstrip patch antenna," *IEEE Trans. Antennas Propag.*, Vol. 60, No. 5, 2151–2156, May 2012.
3. Hazra, R., C. K. Ghosh, and S. K. Parui, "Effect of different semi conductive substrate materials on a P-shaped wearable antenna," *Int. J. of Adv. Res. in Comp. and Comm. Eng. (IJARCCE)*, Vol. 2, No. 8, 3071–3074, 2013.
4. Xi, J., H. Zhu, and T. T. Ye, "Exploration of printing-friendly RFID antenna designs on paper substrates," *IEEE Int. Conf. on RFID*, 38–44, April 2011.
5. Trajkovikj, J., J. F. Zurcher, and A. K. Skrivervik, "Soft and flexible antennas on permittivity adjustable PDMS substrates," *Loughborough Ant. and Prop. Conf.*, 1–4, November 2012.
6. Gunasekaran, S., R. K. Natarajan, A. Kala, and R. Jagannathan, "Dielectric studies of some rubber materials at microwave frequencie," *Ind. J. Pure and APhys.*, Vol. 46, 73–737, October 2008.
7. Ganchev, S. I., J. Bhattacharyya, S. Bakhtiari, N. Qaddoumi, D. Brandenburg, and R. Zaughi, "Microwave diagnosis of rubber compounds," *IEEE Trans. on Microw. Theory and Tech.*, Vol. 42, No. 1, 18–24, January 1994.
8. Al-Hartomy, O. A., F. Al-Solamy, A. Al-Ghamdi, N. Dishovsky, V. Iliev, and F. El-Tantawy, "Dielectric and microwave properties of siloxane rubber/carbon black nano-composites and their correlatio," *Int. J. Polymer Sc.*, Vol. 2011, 2011.
9. Oliveira, F. A., N. Alves, J. A. Giacometti, C. J. L. Constantino, L. H. C. Mattoso, A. M. O. A. Balan, and A. E. Job, "Study of the thermomechanical and electrical properties of

conducting composites containing natural rubber and carbon black," *J. Appl. Polym. Sci.*, Vol. 106, No. 2, 1001–1006, 2007.

10. Ohira, K., "Development of an antenna material based on rubber that has flexibility and high impact resistance," *NTN Tech. Rev.*, No. 76, 2008.
11. Alias, N. A. L., N. A. M. Affendi, Z. Awang, M. T. Ali, and A. Samsuri, "Preliminary studies on the use of natural rubber in the design of flexible microstrip antennas," *2013 IEEE Int. RF Microw. Conf.*, 454–459, Penang, December 2013.
12. Affendi, N. A. M., N. A. L. Alias, Z. Awang, M. T. Ali, and A. Samsuri, "Microwave non-destructing testing of rubber at X-band," *2013 IEEE Int. RF Microw. Conf.*, 333–337, Penang, December 2013.
13. *Basics of Measuring the Dielectric Properties of Materials*, Keysight Technologies ANote, Lit. No. 5989-2589EN, April 27, 2015.
14. Balanis, C. A., "Microstrip antenna," *Antenna Theory: Analysis and Design*, 2nd edition, Chap. 14, 737, 760–762, John Wiley & Sons Ltd, 1997.
15. Carver, K. R. and J. Mink, "Microstrip antenna technology," *IEEE Trans. Antennas Propag.*, Vol. 29, No. 1, 2–24, January 1981.
16. Laheurte, J., "Electrical equivalent circuit of a printed antenna," *Compact Antennas for Wireless Communications and Terminals*, 1st edition, Chap. 5, 62–68, John Wiley & Sons Ltd, 2011.
17. Chen, Z. N. and M. Y. W. Chia, "Planar radiators," *Broadband Planar Antennas*, 1st edition, Chap. 1, 3–31, John Wiley & Sons Ltd, 2006.
18. Baker-Jarvis, J., M. D. Janezic, and D. C. DeGroot, "High-frequency dielectric measurement," *IEEE Trans. Instrum. Meas.*, Vol. 13, No. 2, 24–31, 2010.
19. Pozar, D. M. and D. H. Schaubert, *Microstrip Antennas*, Wiley-IEEE Press, NewYork, 1995.
20. Mäntysalo, M. and P. Mansikkamäki, "An inkjet-deposited antenna for 2.4 GHz applications," *AEU — Int. J. Electron. Commun.*, Vol. 63, No. 1, 31–35, 2009.
21. Sankaralingam, S. and B. Gupta, "Development of textile antennas for body wearable applications and investigations on their performance under bent conditions," *Progress In Electromagnetics Research B*, Vol. 22, 53–71, 2010.
22. Boeykens, F., L. Vallozzi, and H. Rogier, "Cylindrical bending of deformable textile rectangular patch antennas," *Int. J. of Ant. and Prop.*, 1–11, 2012.
23. Reffaee, A. S. A., D. E. El Nashar, S. L. Abd-El-Messieh, and K. N. Abd-El Nour, "Electrical and mechanical properties of acrylonitrile rubber and linear low density polyethylene composites in the vicinity of the percolation threshold," *Int. J. of Mat. in Eng. Applications*, Vol. 30, No. 9, 3760–3769, 2009.
24. Krowne, C. M., "Cylindrical rectangular microstrip antenna," *IEEE Trans. Antennas Propag.*, Vol. 31, No. 1, 194–199, 1983.
25. Bai, Q. and R. Langley, "Textile PIFA antenna bending," *Loughborough Ant. and Prop. Conf.*, 1–4, 2011.
26. Kumar, V., "Radiation pattern of omnidirectional conformal microstrip patch antenna on cylindrical surface," *Int. J. of Emerging Tech. and Adv. Eng.*, Vol. 3, 483–487, February 2013.
27. Katehi, P. B. and N. G. Alexopoulos, "On the effect of substrate thickness and permittivity on printed circuit dipole properties," *IEEE Trans. Antennas Propag.*, Vol. 31, No. 1, 34–38, January 1983.
28. Anaekwe, I., et al., "The effect of curvature adaptation on 2.45 GHz rectangular patch antennas," *IEEE TENCON Spring Conf.*, 123–127, April 2013.
29. Mansor M. M., et al., "A 2.45 GHz wearable antenna using conductive graphene and polymer substrate," *Int. Sym. on Tech. Management and Emerging Tech. (ISTMET)*, 29–32, May 2014.
30. Kellomaki, T., et al., "Bendable plaster antenna for 2.45 GHz applications," *Loughborough Ant. and Prop. Conf.*, 453–456, November 2009.